Photogrammetric Measurement to One Part in a Million

Clive S. Fraser
Geodetic Services, Inc., 1511 South Riverview Drive, Melbourne, FL 32901

ABSTRACT: Industrial photogrammetric measurement to accuracies of 1 part in 1,000,000 of the size of the object is discussed. Network design concepts are reviewed, especially with regard both to the relationships between the first- and second-order design phases and to minimization of the influences of uncompensated systematic error. Photogrammetric system aspects are also briefly touched upon. The network optimization process for the measurement of a large compact range reflector is described and results of successive alignment surveys of this structure are summarized. These photogrammetric measurements yielded three dimensional (3D) coordinate accuracies surpassing one part in a million.

INTRODUCTION

OVER THE LAST DECADE close-range photogrammetry has developed into a mature three-dimensional (3D) coordinate measurement technology. Photogrammetric systems have been tailored for applications as diverse as architectural and archaeological mapping, and the measurement of both aircraft assembly tooling and large engineering structures. Within each broad field of endeavor a finite range of measurement accuracy specifications generally applies. In proportional terms, mapping accuracies of 1 part in 500 of the dimension of an archaeological site may be quite tolerable, yet for high precision application in the aircraft industry photogrammetric systems must yield measurement accuracies of 1 part in 100,000 and better. In the author's experience one area of application stands apart for its stringent precision requirements: the alignment and surface conformity surveys of microwave antenna and optical telescope reflectors.

In reviewing the development of close-range photogrammetry during the past 30 years, it is clear that the initial impetus for systems based on the principles of analytical, monoscopic/convergent photogrammetry came from the requirement to measure and align reflector surfaces of microwave antennas (e.g., Brown, 1962; Forrest, 1966; Kenefick, 1971). At the outset, the antennas were invariably large outdoor communications dishes or radio telescopes. Yet over the years smaller space-borne reflectors, deployable antennas, and optical reflectors have also lent themselves to measurement by photogrammetry (e.g., Merrick et al., 1986; Fraser, 1986; Gustafson, 1990). Accompanying new developments in antenna technology has been the requirement for ever more accurate surface alignment and calibration, and once again there is an impetus to further develop the accuracy capabilities of close-range photogrammetry.

It has only been a few years since this author, for one, talked of measurement accuracies of 1 part in 500,000 as being "within the state-of- the-art." This was effectively a roundabout way of saying that, although photogrammetrists viewed this as feasible, no one had come forward with an object which needed to be photogrammetrically measured to such a tolerance. This situation changed only recently with the development of large compact range antennas. Both Geodetic Services, Inc. (GSI) and a few users of GSI's STARS photogrammetric system have now carried out alignment surveys on reflectors as large as 22m in diameter to accuracies surpassing 1 part in 500,000; i.e. the determination of surface point coordinates to a standard error of 0.04 mm or better over 20m.

The successful carrying out of 3D coordinate measurements to such accuracy requires specialized equipment and techniques: large-format cameras of medium to long focal length are mandatory, as is sub-micrometre image coordinate measurement. Moreover, strong photogrammetric networks employing high convergence angles and imaging configurations of tens of photographs are necessary, along with photogrammetric triangulation utilizing a self-calibrating bundle adjustment (e.g., Fraser, 1986). Photogrammetry, it must be recalled, is an optical triangulation technique. The fundamental observables are angles: the measurement of an (x,y) image coordinate pair on a photograph yields two orthogonal angle observations, in the same way that directions are the basic observables with a theodolite. When we recall that one second of arc (1") is equivalent to a linear proportional measuring resolution of 1 part in 206,000, we can easily infer that photogrammetric measurement to 1 part in 500,000 and beyond requires effective angular precision of well below 1". That photogrammetry has attained this goal is a remarkable achievement.

The purpose of this paper, however, is not to dwell on photogrammetric accuracies at the one part in several hundred thousand level. Instead, we will consider a recent series of alignment measurements of a large compact range antenna in which object point coordinate standard errors of 1 part in 1,000,000 and better were repeatedly achieved. The photogrammetric system utilized for the measurements was the standard STARS system with the large-format CRC-1 camera and the AutoSet-2 sub-micrometre automatic monocomparator. The components of STARS have been fully described elsewhere (Brown, 1984; 1987; Fraser and Brown, 1986) and here we will focus our discussion primarily on the network design aspects which must be addressed if one is to measure 500 target points on a 15- by 17-m surface to an accuracy of better than 20 micrometres (μm). Following a review of salient network design and optimization aspects, the design process for the compact range antenna will be discussed and the measurement results summarized. For an account of the operational aspects of the reflector measurement project, the reader is referred to Brenner and Gustafson (1991).

CONCEPTS OF NETWORK DESIGN

We commence our review of network design concepts at a familiar starting point, the linear functional and stochastic model of the self-calibrating bundle adjustment, which can be written as

$$\begin{aligned} \mathbf{v} &= \mathbf{A}\mathbf{x} - \mathbf{l} \\ \mathbf{C}_l &= \sigma_o^2 \mathbf{P}^{-1}, \end{aligned} \tag{1}$$

where $\mathbf{l}$, $\mathbf{v}$, and $\mathbf{x}$ are the vectors of observations, residuals, and

PHOTOGRAMMETRIC ENGINEERING & REMOTE SENSING,
Vol. 58, No. 3, March 1992, pp. 305–310.

0099-1112/92/5803-305$03.00/0

unknown parameters, respectively; **A** is the design or configuration matrix; $\mathbf{C}_l$ is the covariance matrix of observations; **P** is the weight matrix; and σ_o^2 is the variance factor. In carrying out a network design optimization, the target functions typically apply only to object space *XYZ* coordinates and/or functions of these coordinates. Thus, it is useful to partition **x** into two groups of parameters:

$$\mathbf{x} = \begin{pmatrix} \mathbf{x}_1 \\ \mathbf{x}_2 \end{pmatrix} \tag{2}$$

Here, $\mathbf{x}_1$ comprises the parameters of camera exterior and interior orientation as well as the additional parameters for self-calibration, and $\mathbf{x}_2$ comprises the *XYZ* object point parameters. With this partitioning scheme the normal equations of the least-squares bundle adjustment take the form

$$\begin{pmatrix} \mathbf{A}_1^T\mathbf{P}\mathbf{A}_1 & \mathbf{A}_1^T\mathbf{P}\mathbf{A}_2 \\ \mathbf{A}_2^T\mathbf{P}\mathbf{A}_1 & \mathbf{A}_2^T\mathbf{P}\mathbf{A}_2 \end{pmatrix} \begin{pmatrix} \mathbf{x}_1 \\ \mathbf{x}_2 \end{pmatrix} = \begin{pmatrix} \mathbf{A}_1^T\mathbf{P}\mathbf{l} \\ \mathbf{A}_2^T\mathbf{P}\mathbf{l} \end{pmatrix} \tag{3}$$

In the normal course of a photogrammetric network design, three of four classification stages need to be addressed as detailed in Fraser (1984, 1989). These are Zero-Order (ZOD), First-Order (FOD), and Second-Order Design (SOD). ZOD deals with the datum problem, FOD with the configuration or geometry problem, and SOD with the weight problem. Fortuitously, in close-range photogrammetric networks which employ strong multi-station convergent imaging configurations, we generally need explicitly consider only the latter two of these three design optimization stages. The ZOD problem is neatly side-stepped through Limiting Error Propagation (LEP) whereby the covariance matrix of minimum trace is given approximately by

$$\mathbf{C}_2 = \sigma_o^2 \, (\mathbf{A}_2^T \, \mathbf{P} \, \mathbf{A}_2)^{-1} \tag{4}$$

As shown in Fraser (1987), the covariance matrix $\mathbf{C}_2$ of object point *XYZ* coordinates obtained using Equation 4 is the same for all practical purposes as that determined using an inner-constraint, free-network solution of the normal equations (Equation 3). Of central importance from a practical standpoint is that Equation 4 yields minimum mean variance $\bar{\sigma}_c^2$. That is, optimum mean precision for the *XYZ* coordinates of object points is obtained:

$$\bar{\sigma}_c^2 = \text{tr } \mathbf{C}_2 / 3n \rightarrow \text{minimum} \tag{5}$$

Here, n is the number of points and tr the trace operator.

Associated with each observation of an (x,y) image coordinate pair on the monocomparator is the covariance matrix

$$\begin{pmatrix} \sigma_x^2 & \sigma_{xy} \\ \sigma_{xy} & \sigma_y^2 \end{pmatrix}$$

Within the bundle adjustment of the STARS system, the off-diagonal term σ_{xy} is included to account for short-period film unflatness or emulsion bumpiness which is pseudo-random in character (Brown, 1986). The magnitude of this term is typically quite small for long focal length lenses, but assumes more significance for lenses of wider angle. It is common practice in analytical close-range photogrammetry to implicitly assume that the covariance between image coordinate observations due to film unflatness is negligible, i.e., that $\sigma_{xy} = 0$. Although such an assumption should only be made with caution, the net result is that the network design stages of FOD and SOD are made a little easier to visualize. Hence, we shall also follow this course in the present discussion, even though the covariance propagation used to produce the estimates of precision reported for all simulated and real photogrammetric networks for the compact range reflector measurement have utilized a σ_{xy} value based on a realistic standard error of emulsion bumpiness of 0.003 mm.

For practical purposes, image coordinate measurement precision is taken to be the same for x and y. Thus, σ_x and σ_y can be replaced by a single value which we will call σ. Upon substitution of σ into Equation 4, along with $\sigma_{xy} = 0$ and a variance factor value of one, the expression for $\mathbf{C}_2$ takes the following form:

$$\mathbf{C}_2 = \sigma^2 \, (\mathbf{A}_2^T\mathbf{A}_2)^{-1} \tag{6}$$

In this equation FOD is distinguished by the design matrix product $(\mathbf{A}_2^T\mathbf{A}_2)$ and SOD by σ^2. We note that SOD here provides no more than a scaling for the covariance matrix of the parameters. The separation of SOD and FOD represented by Equation 6 is by no means complete, however. Consider a network of say four camera stations, with its associated covariance matrix $\mathbf{C}_2$. Now, let us assume that instead of one, two photographs are taken at each station. The result will be a simple scaling of $\mathbf{C}_2$ by the factor 0.5 (Fraser, 1984). But was this a change in FOD or SOD? As it turns out, it can be interpreted as either, for the effective scaling of $(\mathbf{A}_2^T\mathbf{A}_2)$ due to the "better" configuration or geometry of triangulation could be matched by the simple assumption of multiple image coordinate observations. Two independent (x,y) coordinate observations will result in an observational variance which is half the corresponding figure for the single reading. Thus, Equation 6 can be extended as follows:

$$\mathbf{C}_2 = \frac{\sigma^2}{k} \, (\mathbf{A}_{2b}^T\mathbf{A}_{2b})^{-1} \tag{7}$$

where $\mathbf{A}_{2b}$ is the design matrix for the "basic" configuration and k is the number of photographs taken at each station of this basic network. As we shall see in the following section, the multiple photographs indicated by k need not be taken either at or very near to the camera stations of the basic network for Equation 7 to remain valid. One proviso though is that this network be of optimal geometric strength; that is, the additional camera stations should not significantly improve on the triangulation geometry represented by the basic network.

This basic network idea has the potential of greatly simplifying the early planning and design stages for a high-precision photogrammetric survey, especially when coupled with the approximate formula

$$\bar{\sigma}_c = q \, S \, k^{-0.5} \, \sigma \tag{8}$$

which was introduced in Fraser (1984) in a slightly different form. Here, S is the scale number (mean camera-to-object distance divided by the focal length) and q is a geometric factor whose value for strong multi-station convergent networks of say four to eight camera stations is likely to be in the range of 0.4 to 0.8.

DESIGN CONSIDERATIONS FOR THE REFLECTOR

In designing an optimal camera station layout for the low curvature surface of the compact range reflector the logical first step is to settle on a suitable image scale, i.e., S in Equation 8. Two aspects are worthy of consideration here, one of which relates directly to accuracy, the other more to practicability. On the practical side, it is beneficial to choose an imaging configuration that allows each photograph to "see" all object target points. Such an arrangement usually also assists in the quest for homogeneity of measurement precision throughout the target field.

From an accuracy optimization point of view, it is necessary to adopt the longest practicable focal length for the camera. Given that the precision of image coordinate measurements is

generally fixed *a priori*, the only way to substantially enhance the angular resolution, and therefore accuracy, of the camera system is to increase focal length. Accompanying such a move, of course, is a decrease in camera field of view, and so a compromise is generally sought.

With the large-format camera, CRC-1, the longest focal-length lens in routine use is 240 mm. If a 1-μm image coordinate accuracy can be maintained, then the CRC-1 with a 240-mm lens will display an angular resolution of better than 1" throughout its 50° by 50° angular field. (It will be shown later that angular accuracies of around half a second are readily attainable with the CRC-1 in conjunction with the AutoSet-2 monocomparator.) Taking into account both the need to maximize image scale and the desirability of having all targets imaged in any one photograph, a stand-off distance of 18.5m from the reflector was chosen. This distance gives rise to an average scale number of $S = 77$.

Once the scale number has been established, the next step is to select an appropriate imaging geometry. To optimize triangulation accuracy at each target, the first logical step in the present instance is to maximize the convergence angles in both the *XZ* and *YZ* coordinate planes. As is often the case, however, there are physical constraints imposed by the height and width of the building containing the reflector, as indicated in Figure 1. At a camera distance of 18.5m from the object, the maximum possible convergence angle in the *XZ* plane is close to 90°, whereas the corresponding figure for the *YZ* plane is about 55°. With the basic four-station network indicated by the solid dots in Figure 1, the best possible optical triangulation geometry is essentially realized.

From the discussion in the previous section, we would anticipate that the addition of camera stations to this network would in most respects be more of an SOD contribution than one of first-order. The improved object point precision which would accompany the use of additional camera station positions will come not so much from an enhancement of basic geometric strength, but more from the fact that additional photographs will be providing a scaling of image coordinate precision in accordance with Equations 7 and 8. This characteristic can be illustrated by considering two network geometries. The first is the four-station arrangement just discussed and the second involves the addition of two extra stations, as indicated by the open circle in Figure 1b.

With an *a priori* image coordinate standard error of 1 μm, the *XYZ* coordinate standard errors (RMS values) obtained from the covariance matrices $\mathbf{C}_2$ for the two networks are as shown in Table 1. The *q*-value from Equation 8 associated with the four-station network is 0.66. Substitution of this value back into Equation 8 with a *k* value of 1.5 (the ratio of six stations over four) yields $\bar{\sigma}_c = 41$ μm, i.e. the identical value to that obtained using the covariance matrix $\mathbf{C}_2$. From the standpoint of variance propagation alone, this finding has significance for it implies that, once a strong basic network is in place (four stations in four logical locations in the present case), there is not much to be gained by proceeding further with an FOD analysis. The addition of further camera station positions is closely akin to simply taking more exposures within the basic network, which is an SOD operation.

There are some practical reasons, however, for not proceeding along the course just outlined. First, not all objects lend themselves to measurement within basic networks of relatively few camera stations; the reflector, it has to be said, constitutes a very straightforward design exercise. Second, and much more important, variance propagation is not the only issue here. There is the question of systematic error in addition to the influence on network geometry of random observational errors.

Within a self-calibrating bundle adjustment, maximum fidelity is aimed for in the functional model. But over and above the imaging perturbations which can be successfully compensated for deterministically, there are systematic errors which do not readily lend themselves to modeling. These may be invariant from photo to photo such as imperfections in the rotational symmetry of lens surfaces, or vacuum platen unflatness. Alternatively, systematic errors may assume a different, yet non-

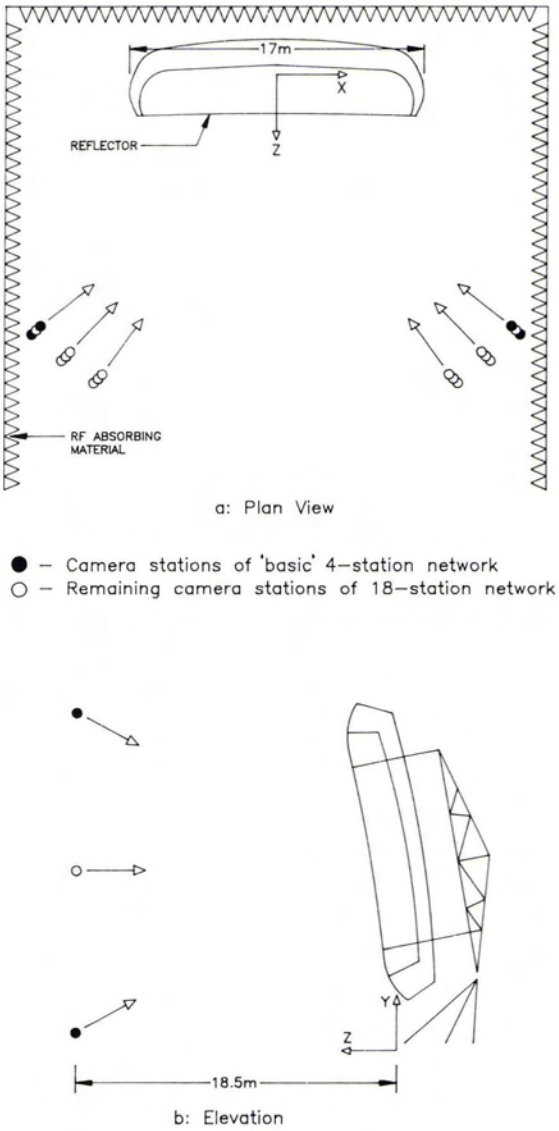

FIG. 1. Camera station configuration for the reflector measurements.

TABLE 1. RMS VALUES OF OBJECT POINT COORDINATE STANDARD ERRORS, IN MICROMETRES, OBTAINED FOR THE TWO BASIC NETWORK DESIGNS, WITH A σ-VALUE OF 1 μM.

	Precision			
Network	$\bar{\sigma}_X$ (range)	$\bar{\sigma}_Y$	$\bar{\sigma}_Z$	$\bar{\sigma}_c$
4-station	53 (53-56)	46 (43-48)	53 (49-60)	51
6-station	43 (43-46)	36 (32-38)	43 (39-51)	41

random, character in each photograph. Examples here might include film deformation, the unflatness of film emulsion, minor instability of the camera's interior orientation, and even specific target characteristics which adversely influence precise centroiding.

Perhaps the most effective way to minimize the parameter biases caused by uncompensated systematic errors is to randomize the error as much as possible. Because such errors may be either common to particular local areas on an image, or have components which are radially dependent, it is beneficial to vary image point locations both through rolling the camera about its axis for multiple exposures at a single station (this is not done to enhance the recovery of interior orientation parameters alone), and through altering camera position. The latter action also serves to lessen the influence of target induced errors which are directionally invariant.

Beyond the systematic errors which defy modeling, there are those which are routinely accommodated, for example, lens distortion and perturbations to the interior orientation. All such errors manifest themselves as changes to image point position, and so to best model their influence we would normally seek the broadest achievable distribution of image point locations to maximize the signal to be modeled. This is another good reason for incorporating additional camera station positions in a network rather than the alternative of relying on the equivalent number of multiple exposures at relatively few stations.

A NETWORK TO YIELD 1:1,000,000 ACCURACY

Having digressed a little to again touch upon the interrelation of FOD and SOD, we return to the task of designing a network for the compact range reflector. The stated accuracy requirement for all but the outer regions and skirt panels of the 15-m by 17-m reflector was for a $\bar{\sigma}_z$-value of 18 μm or better. By a simple recasting of Equation 8, an expression for k, the number of photographs per station, is obtained:

$$k = (q\ S\ \sigma / \bar{\sigma}_c)^2 \qquad (9)$$

The following values can now be substituted into Equation 9: $q = 0.66$ for the four-station geometry, $\bar{\sigma}_c = \bar{\sigma}_z = 18$ μm, $S = 77$, and $\sigma = 1$ μm. This produces a k-value of 8, which implies that a network of 32 photographs would be the minimum required to yield the desired precision.

As it happens, a six-photo network was chosen as the basic imaging configuration. Whereas the two central stations (the open circle in Figure 1b) do not enhance the FOD *per se*, they have been adopted for both practical reasons (the cherrypicker had to visit the upper and lower positions anyway) and for the less tangible reasons regarding unmodeled systematic error influences which were alluded to above. Equation 9 can now be re-applied, this time with $q = 0.55$ for the six-photo geometry. The resulting k-value, rounded up to the nearest integer, is 6. Thus, the final network needs to comprise 36 photographs.

Prior to computing $\bar{\sigma}_z$ from the covariance matrix $\mathbf{C}_2$ to confirm that the desired object point precision would be attainable, a further modification to the network was made. Instead of utilizing one vertical line of three stations on each side of the reflector, with six photos per station, it was decided to employ three vertical lines of three stations, as shown in Figure 1a, with two exposures per station. A full simulation of this network, with an *a priori* σ-value of 1 μm, yielded the precision indicated in Table 2. The reason that the $\bar{\sigma}_z$ value is a few micrometres higher than the estimate obtained using Equation 9 is likely a function of the decreased convergence angle which accompanies the addition of the four new vertical lines of photography (open circles in Figure 1a) in the 18-station network. The contribution of the σ_{xy} covariance term is also a minor factor in this difference.

TABLE 2. RMS VALUES OF OBJECT POINT COORDINATE STANDARD ERRORS, IN MICROMETRES, OBTAINED IN THE SIMULATED 36-PHOTO NETWORK WITH A σ VALUE OF 1 μM.

Network	Precision $\bar{\sigma}_X$ (range)	$\bar{\sigma}_Y$	$\bar{\sigma}_Z$	$\bar{\sigma}_c$
18 stations, 2 exposures per station	15 (15-18)	15 (13-15)	20 (20-25)	17

The Z-coordinate precision listed in Table 2 falls short of requirements by about 10 percent. To overcome this deficiency we can turn to SOD, i.e., to a simple scaling of σ and therefore $\mathbf{C}_2$. To reach $\bar{\sigma}_z = 18$ μm, a σ-value for image coordinate measurements of 0.9 μm would be required. This figure is routinely improved upon in bundle adjustments of CRC-1 photographs when film measurement is carried out on the AutoSet monocomparator. In any design process, however, it invariably does not hurt to err on the conservative side; hence, at GSI we routinely use a σ-value of 1 μm for network simulations. It is worth recalling here that the film measurement accuracy of AutoSet is close to 0.3 μm; the remaining half-micrometre component of the triangulation misclosure is attributable to the unmodeled systematic error influences for which a minimization (and randomization) is sought, both through camera rotation and variations to a basic network geometry.

With a fair degree of confidence that a σ-value of 0.9 μm or better could be maintained, we adopted the network geometry shown in Figure 1 for the multiple measurements of the front surface of the compact range reflector. Expressed in proportional terms, this was to be a photogrammetric measurement to better than 1 part in 1,000,000.

MEASUREMENT RESULTS

In total, nine photogrammetric measurements were made of the antenna during the final mechanical alignment phase. Of these, five will be discussed here, namely, successive measurements of the central and intermediate front section panels of the reflector following physical re-alignments. The remaining four surveys consisted of one to determine initial surface conformity following the theodolite alignment phase, and three to determine alignment of the intermediate and/or skirt panels at the top, bottom, and two sides of the antenna. As is indicated in Figure 1, the reflector incorporated wraparound panels at its edges which extended back some 3m or so from the front surface. These skirt panels presented a challenging photogrammetric survey task, and their measurement to 85 μm accuracy required networks of 100 or so photographs taken with a CRC-1 fitted with a wide angle lens (Brenner and Gustafson, 1991).

Of the five surveys considered, two encompassed the entire front section of the reflector, whereas the other three concentrated on the central 27 panels which constituted an area of about 11m by 8.5m. On the front section as a whole there were just over 500 photogrammetric retrotargets, with 216 being on the central panels (eight per panel). For all five measurements, the basic network geometry discussed in the previous section was adopted, though with one modification which had only a minor impact on precision. Due to visibility concerns in the areas adjacent to two theodolite support towers, two more camera stations were added, with two photographs being taken at each. The addition of these extra photographs did not influence the geometry of the basic 18-station configuration indicated in Figure 1 to a measurable extent, and only about a 5 percent or 1 μm improvement in coordinate standard error was anticipated using the k-factor in Equation 8.

The *XYZ* coordinate precision obtained in the five 40-photo photogrammetric measurements is summarized in Table 3. The covariance matrices $\mathbf{C}_2$ for the networks were obtained through a full inversion of the normal equation matrix, Equation 3, as opposed to using LEP. Of principal note is that in all cases object point coordinate standard errors of better than 1 part in 1,000,000 were achieved. Moreover, the two networks covering the full 21.5-m diameter reflector face yielded results which were fully consistent with expectations from the network design.

One question that arises from the results listed in Table 3 concerns the disparity between the triangulation misclosures that accompany measurement of the full front versus those for the surveys of the central region. In the former case misclosures at close to 0.9 μm or 0.8″ are seen, whereas in the latter the corresponding figures are 0.6 to 0.7 μm or about 0.6″. Noteworthy in the search for an explanation for this difference is the fact that the full image format of the CRC-1 is employed in the network covering the 500 targets, whereas only the central area out to a radial distance of about 8 cm on the film is utilized in the network of 220 points.

That vectors of image coordinate residuals show systematic growth trends with increasing radial distance is a well-known characteristic in analytical photogrammetry. A number of factors can contribute to this phenomenon. Thermal loading on structures as large as the compact range reflector can readily induce periodic changes in shape. Thus, the object may not remain shape invariant during the period of photography. Such behavior can be expected to more adversely influence the measurement of the larger area of the reflector. Moreover, film bumpiness and platen unflatness influences become more pronounced with increasing radial distance, a factor which could certainly account for induced film measurement errors of sufficient magnitude to explain the 0.2-μm misclosure disparity between the two network groups in Table 3. Whatever the major contributing factor is, it seems fair to say that the source of this radially dependent image coordinate error component is beyond functional modeling for all practical purposes. The stochastic influence of a smaller *a posteriori* variance factor for the photogrammetric triangulation is of course significant for it provides a scaling of the covariance matrix $\mathbf{C}_2$. In Table 3 it can be seen that the reduction of the triangulation misclosure in the latter three photogrammetric networks matches closely the percentage reduction in the principal dimension of the target field, thus providing a measure of uniformity in the proportional accuracies obtained.

TABLE 3. NETWORK PRECISION OBTAINED IN FIVE MEASUREMENTS OF THE COMPACT RANGE REFLECTOR. STANDARD ERROR UNITS ARE MICROMETRES.

Network	Precision $\bar{\sigma}_X$	$\bar{\sigma}_Y$	$\bar{\sigma}_Z$	$\bar{\sigma}_c$	$\bar{\sigma}_p/D$	Triangulation Misclosure (μm, ″)
Central + Intermediate Panels, 512 pts. D = 21.5m						
Meas. 1	13	13	18	15	1:1,190,000	0.91, 0.8
Meas. 2	13	13	18	15	1:1,190,000	0.91, 0.8
Central Panels Only, 220 pts, D = 13.8m						
Meas. 1	11	10	13	11	1:1,060,000	0.70, 0.6
Meas. 2	10	10	13	11	1:1,060,000	0.69, 0.6
Meas. 3	10	9	13	11	1:1,060,000	0.63, 0.5

CONCLUDING REMARKS

An issue which can arise in a photogrammetric survey to extremely high precision is accuracy verification. This presents some practical difficulties. The reason photogrammetry was employed in the compact range reflector alignment was that no competing technology was readily suitable for the task. Thus, there is no easy means to externally verify photogrammetric accuracies in a comprehensive fashion. It is of course common practice to employ redundant length scale information to verify measured point-to-point distances, and also to make use of shim targets to independently assess relative Z-coordinate accuracy. But, for an overall quality control measure, internal accuracy indicators within the photogrammetric network, namely the covariance matrix $\mathbf{C}_2$ of object point coordinates must be relied upon.

For such a reliance on measures of *XYZ* coordinate precision, we require network designs which display high internal and external reliability. Fortunately, in this case reliability is not an issue; the network geometry is strong and the triangulation of each target is 38 times overdetermined when the point is imaged on 40 photographs (i.e., an observational redundancy per multi-ray point intersection of 77). In such circumstances there can be a very high degree of confidence that internal measures of precision are valid estimates of the external accuracy of the measured *XYZ* coordinate data.

The achievement of 3D coordinate measurement accuracies of 1 part in 1,000,000 breaks new ground for industrial photogrammetry. The measurement example of the compact range reflector presented illustrates that, with a suitable close-range photogrammetric system (both hardware and software) and due attention to network design optimization, it is possible today to achieve spatial measurement resolution which is fully an order of magnitude higher than that which represented the state-of-the-art only a decade ago.

REFERENCES

Brenner, M., and P.C. Gustafson, 1991. Alignment and Measurement of a Large Blended Compact Range Reflector. Presented paper, 13th Annual Meeting and Symposium of the Antenna Measurement Techniques Association (AMTA), Boulder, 7–11 Oct.

Brown, D.C., 1962. *Precise Calibration of Surfaces of Large Radio Reflectors by Means of Analytical Photogrammetric Triangulation.* Research and Analysis Technical Report #10, Instrument Corp. of Florida, Melbourne.

———, 1984. A Large Format, Microprocessor Controlled Film Camera Optimized for Industrial Photogrammetry. Presented Paper, XV Congress of ISPRS, Commission V, Rio de Janiero, June, 29 p.

———, 1986. Unflatness of Plates as a Source of Systematic Error in Close-Range Photogrammetry, *Photogrammetria*, 40:343–363.

———, 1987. AutoSet, An Automated Monocomparator Optimized for Industrial Photogrammetry. Presented Paper, Int. Conf. and Workshop on Analytical Instrumentation, Phoenix, Arizona, 2–6 Nov., 16 p.

Forrest, R.B., 1966. Radio Reflector Calibration. *Photogrammetric Engineering*, 32(1):109–112.

Fraser, C.S., 1984. Network Design Considerations for Non-Topographic Photogrammetry. *Photogrammetric Engineering & Remote Sensing*, 50(8):1115–1126.

———, 1986. Microwave Antenna Measurement by Photogrammetry. *Photogrammetric Engineering & Remote Sensing*, 52(10):1627–1635.

———, 1987. Limiting Error Propagation in Network Design. *Photogrammetric Engineering & Remote Sensing*, 53(5):487–493.

———, 1989. Optimization of Networks in Non-Topographic Photogrammetry. *Non-Topographic Photogrammetry, Second Edition* (S.M. Karara, Ed.), ASPRS, Falls Church, Virginia, Chap. 8, pp. 95–106.

Fraser, C.S., and D.C. Brown, 1986. Industrial Photogrammetry: New

Developments and Recent Applications. *The Photogrammetric Record*, 12(68):197–217.

Gustafson, P.C., 1990. Photogrammetric Surveys of the Mirror Support Cell of the Keck Optical Telescope. *Int. Archives of Photogrammetry & Remote Sensing*, ISPRS, 28(5/1):417–424.

Kenefick, J.F., 1971. Ultra-Precise Analytics. *Photogrammetric Engineering*, 37(11):1167–1187.

Merrick, W.D., F.L. Lansing, F.W. Stoller, and V.B. Lobb, 1986. Precision Photogrammetric Measurements of NASA-JPL 34-M Antenna Reflectors. Presented paper, Montech-86, IEEE Conference on Antennas and Communications, Montreal, October.

(Received 3 May 1991; accepted 10 June 1991)